




Article

Evaluation of Infrared Radiation Combined with Hot Air Convection for Energy-Efficient Drying of Biomass

Hany S. EL-Mesery ^{1,2}, Abd El-Fatah Abomohra ^{3,4,*}, Chan-Ung Kang ⁵, Ji-Kwang Cheon ⁵, Bikram Basak ⁵ and Byong-Hun Jeon ^{5,*}

¹ School of Energy and Power Engineering, Jiangsu University, Zhenjiang 212013, China

² Department of Crop Handling and Processing, Agricultural Engineering Research Institute, Agricultural Research Center, Dokki, Giza 12618, Egypt

³ New Energy Department, School of Energy and Power Engineering, Jiangsu University, Zhenjiang 212013, China

⁴ Botany Department, Faculty of Science, Tanta University, Tanta 31527, Egypt

⁵ Department of Earth Resources and Environmental Engineering, Hanyang University, Seoul 04763, Korea

* Correspondence: abomohra@science.tanta.edu.eg (A.E.-F.A.); bhjeon@hanyang.ac.kr (B.-H.J.)

Received: 14 June 2019; Accepted: 19 July 2019; Published: 22 July 2019



Abstract: Cost-effective biomass drying is a key challenge for energy recovery from biomass by direct combustion, gasification, and pyrolysis. The aim of the present study was to optimize the process of biomass drying using hot air convection (HA), infrared (IR), and combined drying systems (IR-HA). The specific energy consumption (SEC) decreased significantly by increasing the drying temperature using convective drying, but higher air velocities increased the SEC. Similarly, increasing air velocity in the infrared dryer resulted in a significant increase in SEC. The lowest SEC was recorded at 7.8 MJ/kg at an air velocity of 0.5 m/s and an IR intensity of 0.30 W/cm², while a maximum SEC (20.7 MJ/kg) was observed at 1.0 m/s and 0.15 W/cm². However, a significant reduction in the SEC was noticed in the combined drying system. A minimum SEC of 3.8 MJ/kg was recorded using the combined infrared-hot air convection (IR-HA) drying system, which was 91.7% and 51.7% lower than convective and IR dryers, respectively. The present study suggested a combination of IR and hot air convection at 60 °C, 0.3 W/cm² and 0.5 m/s as optimum conditions for efficient drying of biomass with a high water content.

Keywords: biomass drying; convection hot-air; infrared; specific energy consumption; drying time

1. Introduction

The utilization of bio-resources has been widely discussed to replace non-renewable resources such as fossil fuel, which is limited and results in undesirable emissions that largely contribute to climate change and global warming [1]. Waste biomasses have been discussed as a sustainable feedstock for chemicals and energy production. For example, polyhydroxyalkanoates (PHAs) is a biodegradable bio-polyester that can be accumulated by different bacterial cells grown on agro-industrial wastes [2–4]. In addition, the contribution of biomass, as one of the world's major sustainable energy sources [5], in global energy consumption was estimated to reach up to 50% by the year 2050 [6,7]. Biomass can be converted into different types of biofuels through various conversion routes, such as the production of biogas through anaerobic digestion of biomass [8–10], the conversion of algal lipids to biodiesel [11,12], the production of bioethanol through the fermentation of carbohydrates and amino acids [13,14], and crude bio-oil through the thermochemical conversion of the whole biomass [15]. Wang et al. [16] reported that the thermochemical conversion of biomass was a favorable route because it allowed for

the conversion of the whole biomass in a single step. Among different thermochemical conversion methods, fast pyrolysis was reported as a more efficient method due to its relatively higher productivity of crude bio-oil, despite a higher capital investment [17]. One reason for the high cost of pyrolysis and PHAs production is the need for biomass drying before conversion. In addition, the thermal drying of biomass with high moisture content is a critical step for further efficient utilization in direct combustion and gasification [18–20]. Thus, one aspect to enhance the economics of biomass conversion is the application of cost-effective drying as it can significantly reduce the costs associated with handling, transportation, and the conversion process. Drying, or the removal of moisture from biomass, is widely used in agriculture to reduce water activity and slow down the microbial spoilage and deterioration of the product [21–23]. However, drying also significantly concentrates the dry matter and the energy content of the biomass as a mild torrefaction step. The moisture content of the biomass plays a vital role in the stability of the produced bio-oil [24]. The high water content of the crude bio-oil results in phase separation, which is a handicap for fuel applications [25]. Therefore, reducing the water content to below 10% was reported as a crucial factor in achieving a higher conversion rate and bio-oil yield [17].

Cost-effective biomass drying with minimum energy consumption is receiving increasing attention. In recent years, many drying methods have been discussed, from conventional sun drying to modern dryer technologies. Sun drying is a traditional method that is still used as a freely available and cheap method for food drying in most developing countries [26]. However, biomass undergoes a long uncontrolled drying period that affects the biomass composition and the process economy [27]. In recent years, modern fast dryers providing controlled conditions have been used instead of traditional drying. However, such systems are highly energy intensive and often expensive [28], limiting their application in the biofuel industry.

Due to the aforementioned environmental concerns and limited fossil fuel reserves, it is crucial to reduce the total energy consumption in the drying process for cost-effective biomass conversion. Thus, saving the available energy sources by deploying new drying systems with the lowest energy consumption is a challenge [23]. The high energy consumption of hot air convection (HA) systems directed the research towards exploring and designing new drying technologies such as the microwave, infrared (IR), freezing, and vacuum drying, individually or in combination. Heating by means of IR radiation is gaining more popularity than conventional heating methods as it heats products more uniformly, it transfers heat quickly and efficiently, and there are lower processing costs involved [29]. In this context, Onwude et al. [30] reported that the combination of hot air and IR radiation resulted in a synergistic effect, leading to more efficient drying than either individual convective or IR drying.

Different investigations have been conducted to study the conversion efficiency and energy yield of different biomasses [31–35]. However, the literature is still limited to the selection of energy-efficient drying methods based on the specific energy consumption (SEC) and optimization of an energy-efficient dryer for watery biomass feedstock. The main objective of this study was to evaluate and compare three drying technologies using a model watery biomass in order to reduce the drying time and energy consumption. Drying using HA and IR, individually and combined, was investigated. For each system, the drying time and SEC were calculated, and the results were modeled. Finally, a preliminary suggestion for an efficient drying method was made.

2. Experimental System and Methods

2.1. Biomass Feedstock and Experimental System

In the present study, fresh tomato slices were used as a model high water content biomass. Tomato fruits were sliced with a mechanical slicing machine (55600-1, NEMCO Easy Tomato Slicer, Ohio, United States) into slices of 5 ± 0.2 mm thickness. Three measurements using a Vernier caliper were made on each slice to confirm the thickness. The average initial moisture content of the tomato slices was 94.4 ± 1.13 %wt.

Figure 1 shows a schematic diagram of the drying equipment used. A tube type IR heater was installed in the drying chamber of a convection hot-air dryer. Air was blown into the drying chamber using a fan placed opposite two spiral-type electrical heaters, each with a heating capacity of 1.5 kW and connected to an air controller that regulates the air velocity measured (as m/s) using an anemometer (Testo 405 V1, Lenzkirch, Germany) above the tray surface. To measure the air temperature, T-type thermocouples (Testo 925) with an accuracy of ± 1 °C was connected to a data logger.

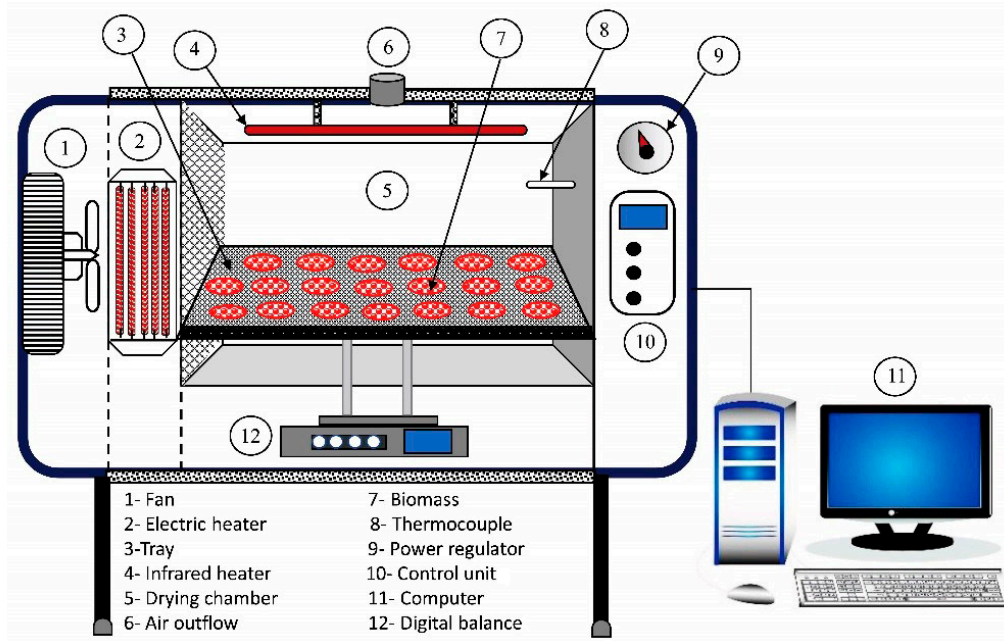


Figure 1. Schematic diagram showing that the drying system used in the present study consisted of a convection hot-air dryer and an infrared radiation dryer.

2.2. Drying Procedure

The dryer was operated at different air velocities of 0.5 m/s, 0.7 m/s, and 1.0 m/s and air temperatures of 50 °C, 60 °C, and 70 °C for convection hot air drying. For IR radiation drying, three intensities (0.15, 0.20, and 0.30 W/cm²) were studied at 25 ± 1 °C, and the three above mentioned air velocities. The combined IR/hot air convection drying was performed by a combination of the aforementioned conditions of radiation intensity, air temperatures, and air velocities. For each experiment, 15 slices weighing between 200–220 g were dried using the three drying methods. A built-in precision balance was used to measure the weight reduction of the samples (Figure 1) with a final moisture content of 5%.

2.3. Specific Energy Consumption

The electrical energy consumed was measured as the total energy consumption (E_T , MJ), including the energy consumed by the IR heaters, the fan, and the electric heater (Equation (1)). By applying the IR dryer, the E_T was defined as the sum of energy consumed by the ventilator fan and the IR heater. Using the combined drying method, E_T was calculated from Equation (1):

$$E_T = E_{IR} + E_F + E_H \quad (1)$$

where E_T , E_{IR} , E_F , and E_H represent (in MJ) the total energy consumption, energy consumed by the IR heaters, the fan, and the electric heater, respectively.

The values of E_T were used to calculate the specific energy consumption (SEC, as MJ/kg of water evaporated) as shown in Equation (2):

$$\text{SEC} = \frac{E_T}{\text{Weight loss (kg)}} \quad (2)$$

2.4. Statistical Analysis

All experiments were repeated three times and the values were represented as the mean \pm standard deviation (SD). SPSS[®] (IBM, v. 20) was used to carry out the statistical analysis by a one-way ANOVA followed by a least significant difference (LSD) test at a probability level of ($P \leq 0.05$). TableCurve 3D V4.0 (SYSTAT Software Inc., San Jose, USA) software was applied to obtain fitting surfaces and prediction equations. More than 25,000 built-in equations based on linear and nonlinear models (e.g., polynomial functions, linear equations, and logarithmic functions) were fitted. TableCurve 3D combines an influential surface fitter with the ability to find the perfect equation to describe the 3D experimental data based on coefficient of determination (R^2), the adjusted determination coefficient (adj R^2) and the fit standard error (Fit Std Err). The finalized design equation with a high determination coefficient was chosen for each experiment.

3. Results and Discussion

One of the main goals in constructing and optimizing an industrial drying process is to determine the shortest time in which the maximum reduction of moisture content in the biomass can be achieved. Therefore, energy consumption, as well as heat and mass transfer, should be inspected during the drying process. The SEC is defined as the energy consumed to evaporate 1 kg of moisture from the biomass [36]. Hence, the optimization of air velocity and air temperature are key parameters for cost-effective drying.

3.1. Hot Air Convection Drying

The drying time required by the hot air convection dryer to reach the target final moisture content of biomass feedstock is represented in Figure 2A which shows that the increase in hot air temperature and air velocity resulted in a significant reduction in drying time. The increasing temperature from 40 to 60 °C resulted in a reduction of the drying time by 22.2%, 21.7%, and 20.8% at 0.5, 0.7, and 1.0 m/s, respectively. Based on the drying temperature (T , °C) and air velocity (V , m/s), the multiple regression analysis of the drying time can be represented by Equation (3) ($R^2 = 0.998$; Adj $R^2 = 0.987$ and Fit Std Err = 9.48) from the 3-D analysis (Supplementary Data, Figure S1).

$$\text{Drying time} = \frac{632.05 - 314.95 \ln T + 39.24(\ln T)^2 + 0.32V}{1 - 0.49 \ln T + 0.06(\ln T)^2 + 0.002V} \quad (3)$$

The reduction in drying time due to the increase in temperature or air velocity is attributed to the enhancement of the evaporation rate [37,38]. The maximum rate of reduction in the drying time was recorded at 50 °C with 0.7 m/s (−10.5 min/C), while air velocity showed much higher impact on the rate of reduction in the drying time and showed its maximum value of −600 min/unit velocity at 50 °C and 0.7 m/s (Supplementary Data, Figure S2). This resulted in a significant reduction in the SEC by increasing the temperature at the same air velocity, while the SEC increased at the same temperature by increasing the air velocity (Figure 2B). The minimum value of the SEC was 45.24 MJ/kg at 60 °C and 0.5 m/s, while, a maximum SEC value of 86.97 MJ/kg was recorded at 50 °C and 1.0 m/s. Therefore, the application of high air velocities during the drying process resulted in higher energy consumption, while increasing air temperature resulted in lower total energy consumption due to the reduced drying time. From a multiple regression analysis (Supplementary Data, Figure S3), the polynomial regression equation (Equation (4)) showed an associated coefficient (R^2) of 0.991.

$$\text{SEC} = \frac{109.7 - 1.7 T + 18.9 V - 38.8 V^2}{1 + 0.01 T - 0.0003 T^2 - 0.7 V} \quad (4)$$

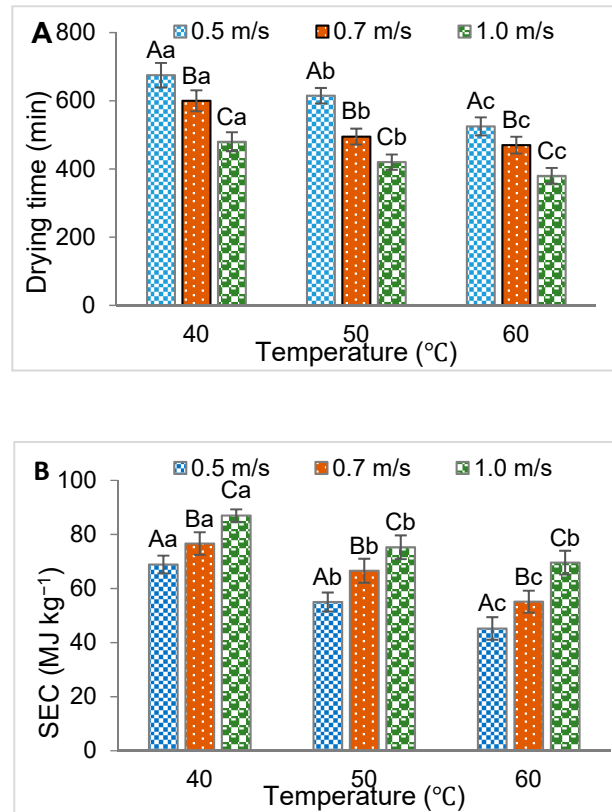


Figure 2. The impact of air velocity and temperature on drying time (A) and specific energy consumption (SEC, B) using a hot air convection dryer. The different capital letters at the same temperature showed significant differences, while different lowercase letters of the same series showed significant differences (at $P \leq 0.05$). The equation 5 model was found to fit the experimental data with an adjusted determination coefficient ($\text{Adj } R^2$) of 0.987, correlation coefficient (R^2) of 0.998 and the fit standard error (Fit Std Err) of 5.68, indicating that the fitness of the selected model is good.

3.2. Infrared Radiation Drying

Throughout the IR drying process, radiation energy is transferred directly to the surface of the biomass without affecting the ambient temperature, which increases the sample temperature, causing the moisture to evaporate [39]. Generally, the drying time increased by increasing the air velocity, while it was decreased by increasing the IR intensity (Figure 3A). The shortest drying time was recorded at 320 min at 0.3 W/cm² IR intensity and 0.5 m/s air velocity. However, increasing the air velocity to 0.7 and 1.0 m/s at the same IR intensity (0.30 W/cm²) resulted in a significant increase in the drying time by 21.9% and 39.1%, respectively, over that at 0.5 m/s. A maximum drying time of 560 min was recorded at the lowest studied IR intensity (0.15 W/cm²) and the highest air velocity (1.0 m/s). This might be ascribed to the cooling effect on the biomass surface by increasing the air velocity [40,41]. However, increasing IR intensity resulted in a significant increase in the temperature of the biomass and the rate of evaporation, leading to a shorter drying time. In this context, previous studies confirmed the increase in the rate of heating and moisture removal of biomass using IR radiation compared to convective drying [42]. In accordance with the present results, Das et al. [43] used IR drying for high moisture paddy and reported that efficient drying occurred in the radiation range of 0.15–0.55 W/m² for four levels of grain bed depths. The higher efficiency of IR drying can be attributed to the high heat

transfer of the biomass, which was reported to be limited in the case of convective drying due to lower thermal conductivity [44]. In addition, Fasina et al. [45] concluded that IR heating could improve the water hydration capacity and functional properties of the biomass. From the results of the multiple regression analyses (Supplementary Data, Figure S4), drying time can be calculated using Equation (5) ($R^2 = 0.998$) based on the air velocity (V , m/s) and intensity of IR radiation (I , W/cm^2).

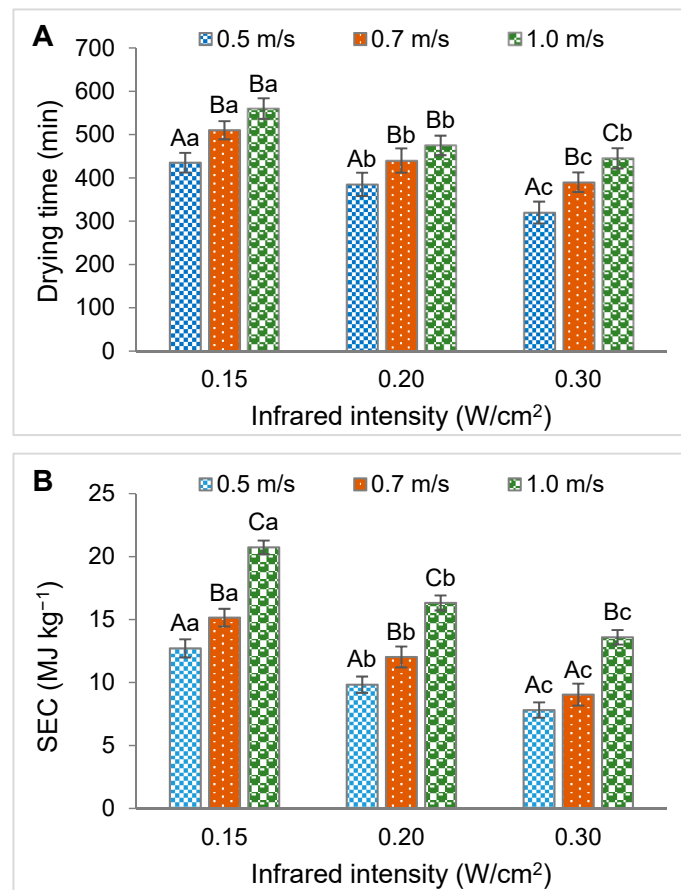


Figure 3. The effect of infrared radiation at different air velocities on the drying time (A) and specific energy consumption (SEC, B). The different capital letters at the same infrared intensity showed significant differences, while different lowercase letters of the same series showed significant differences (at $P \leq 0.05$).

$$\text{Drying time} = \frac{677.8 + 146.3 \ln V + 202.5 \ln I + 0.32 I}{1 + 0.27 \ln V - 0.2(\ln V)^2 + 1.01 I + 0.4(\ln I)^2} \quad (5)$$

Figure 3B shows the SEC using the IR dryer at different air velocities and IR radiation intensities. A minimum SEC of 7.81 MJ/kg was recorded at 0.5 m/s and 0.30 W/cm^2 , while a maximum SEC of 20.73 MJ/kg was noted at 1.0 m/s and 0.15 W/cm^2 . Therefore, increasing radiation intensity with lower air velocity resulted in a significant reduction in the SEC. Since IR has no impact on the surrounding air temperature, the recorded increase in the energy consumption by increasing the air velocity is attributed to the accompanied cooling effect of the applied air to the surface of the biomass which increased the drying time. The multiple regression analysis (Supplementary Data, Figure S5) of the SEC, IR intensity, and air velocity can be represented by Equation (6) with $R^2 = 0.999$ (Adj $R^2 = 0.992$ and Fit Std Err = 0.249).

$$\text{SEC} = \frac{15.87 - 3.2 V - 73.6 I + 114.1 I^2}{1 - 0.94 V + 0.28 V^2 - 0.93 I} \quad (6)$$

3.3. Combined Infrared/Hot Air Convection

The results of applying a combination of IR and hot air convection (IR-HA) methods for biomass drying are shown in Figures 4 and 5. At various studied temperatures, the required drying time showed the same pattern where increasing the air velocity led to a significant increase in the drying time and increasing the IR intensity significantly reduced the drying time (Figure 4). In addition, an increase in temperature led to a significant reduction in the required drying time. Overall, the lowest drying time was recorded at 225 min at the highest applied temperature (60 °C), highest IR intensity (0.30 W/cm²), and lowest air velocity (0.5 m/s) (Figure 4C). This is due to an increase in the temperature of the inner slices by increasing the radiation intensity, which increased the temperature gradient of the surface layer of the biomass and reduced the drying time [46]. The increase in air temperature results in a gradual increase in the temperature of the biomass from the surface to the inside, which enhances the drying efficiency [47–49]. Hence, the internally generated heat by the IR and the hot air flow resulted in a rapid reduction of moisture content due to the diffusion of water to the surface of the biomass, followed by its evaporation [42,50]. The reduction in drying time resulted in a significant reduction in the SEC (Figure 5). The increase of IR intensity and applied temperature led to a reduction of the SEC. With an air velocity of 0.5 m/s at 40 °C, the SEC decreased significantly from 9.53 to 7.01 MJ/kg, while it decreased from 18.95 to 12.91 MJ/kg at 1.0 m/s by increasing the intensity of the IR radiation from 0.15 to 0.3 W/cm² (Figure 5A). In addition, SEC increased when the air velocity was increased at all temperatures and IR intensities studied, which is consistent with the drying time behavior.

The multiple regression analysis for the interaction effect of air velocity and IR intensity on the drying time at different drying temperatures using a combined dryer (IR-HA, Supplementary Data, Figure S6) can be represented by Equations (7)–(9). In addition, the multiple regression analysis of the SEC (Supplementary Data, Figure S7) can be represented by Equations (10)–(12). In addition, the residual plot of minimum drying time and corresponding SEC using the generated equations for the three studied drying systems (Figure 6) showed low residual values, which confirms that the predicted values are in high correlation with the experimental values.

$$\text{At } 40\text{ }^{\circ}\text{C, Drying time} = \frac{301.2 + 425.8 \ln V + 494.7(\ln V)^2 - 0.32 \ln I}{1 + 0.88 \ln V - 1.7(\ln V)^2 + 0.18 \ln I} R^2 = 0.998 \quad (7)$$

$$R^2 = 0.998; \text{Adj}R^2 = 0.987; \text{Fit Std Err} = 4.137$$

$$\text{At } 50\text{ }^{\circ}\text{C, Drying time} = \frac{247.3 + 191.1 \ln V + 14.2 \ln I - 51.8(\ln I)^2}{1 + 0.76 \ln V - 1.4(\ln V)^2 + 1.45(\ln V)^3 + 0.48 \ln I} R^2 = 0.998 \quad (8)$$

$$R^2 = 0.998; \text{Adj}R^2 = 0.970; \text{Fit Std Err} = 4.632$$

$$\text{At } 60\text{ }^{\circ}\text{C, Drying time} = \frac{527.9 - 397.6 \ln V - 651.8(\ln V)^2 - 830 I}{1 - 1.6 \ln V - 2.07(\ln V)^2 - 0.22 I} R^2 = 0.998 \quad (9)$$

$$R^2 = 0.998; \text{Adj}R^2 = 0.989; \text{Fit Std Err} = 4.155$$

$$\text{At } 40\text{ }^{\circ}\text{C, SEC} = 18.2 + 3.5/I - 18.7/V - 0.05/I^2 + 5.56/V^2 - 1.07/(IV) R^2 = 0.991 \quad (10)$$

$$R^2 = 0.996; \text{Adj}R^2 = 0.987; \text{Fit Std Err} = 0.363$$

$$\text{At } 50\text{ }^{\circ}\text{C, SEC} = 22.2 + 3.9/I - 25.9/V - 0.11/I^2 + 7.99/V^2 - 1.17/(IV) R^2 = 0.991 \quad (11)$$

$$R^2 = 0.991; \text{Adj}R^2 = 0.966; \text{Fit Std Err} = 0.584$$

$$\text{At } 60\text{ }^{\circ}\text{C, SEC} = 30.65 + 2.07/I - 34.59/V - 0.03/I^2 + 10.13/V^2 - 0.68/(IV) R^2 = 0.992 \quad (12)$$

$$R^2 = 0.992; \text{Adj}R^2 = 0.969; \text{Fit Std Err} = 0.523$$

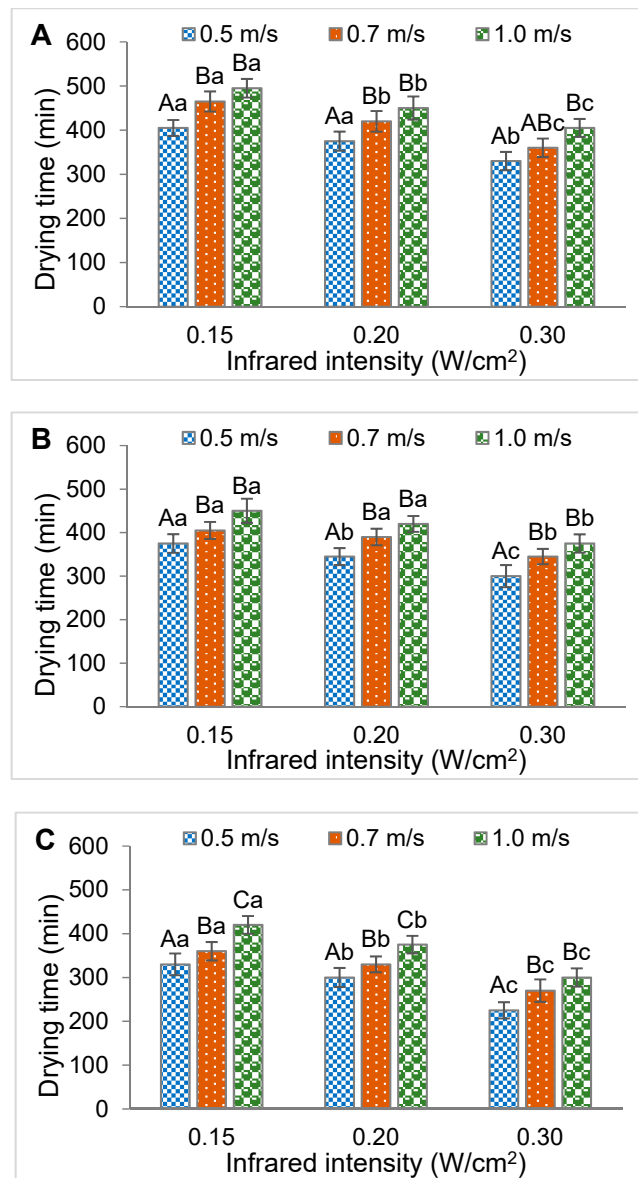


Figure 4. The effect of infrared radiation intensity at different air velocities on the drying time using a combined dryer at 40 °C (A), 50 °C (B) and 60 °C (C). The different capital letters at the same infrared intensity showed significant differences, while different lowercase letters of the same series showed significant differences (at $P \leq 0.05$).

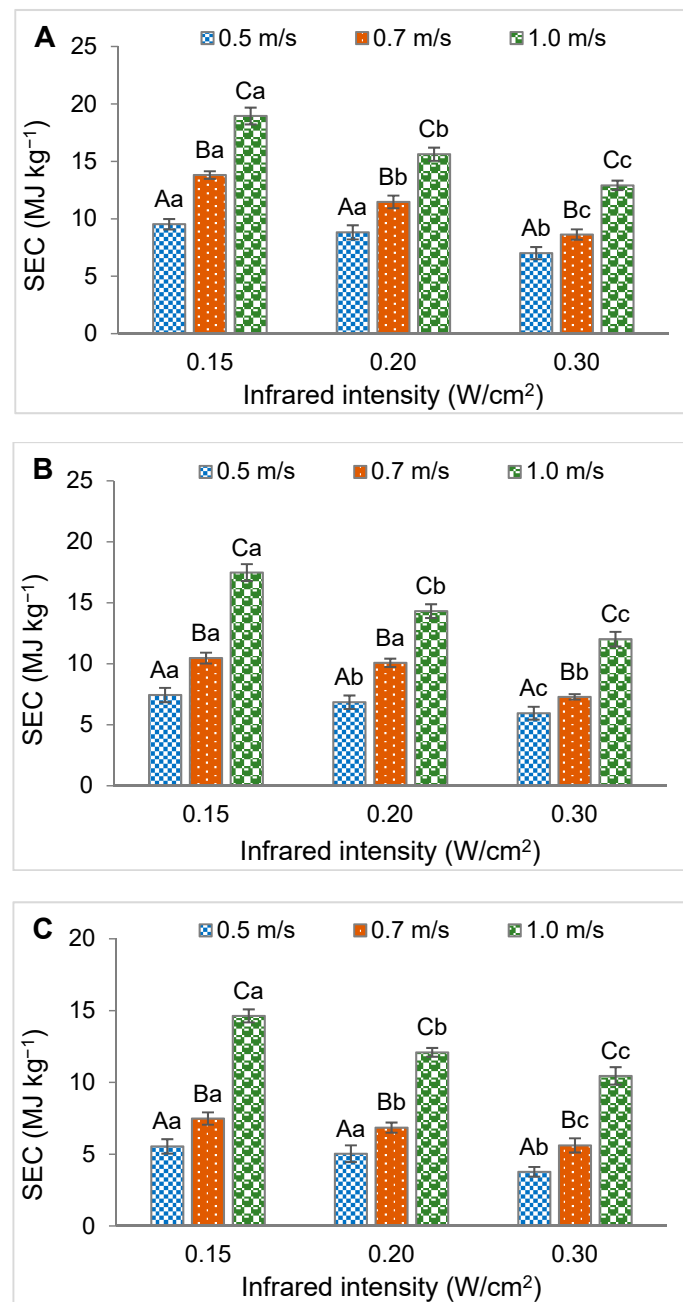


Figure 5. The effect of infrared intensity at different air velocities on the specific energy consumption (SEC) using a combined dryer at 40 °C (**A**), 50 °C (**B**) and 60 °C (**C**). The different capital letters at the same infrared intensity showed significant differences, while different lowercase letters of the same series showed significant differences (at $P \leq 0.05$).

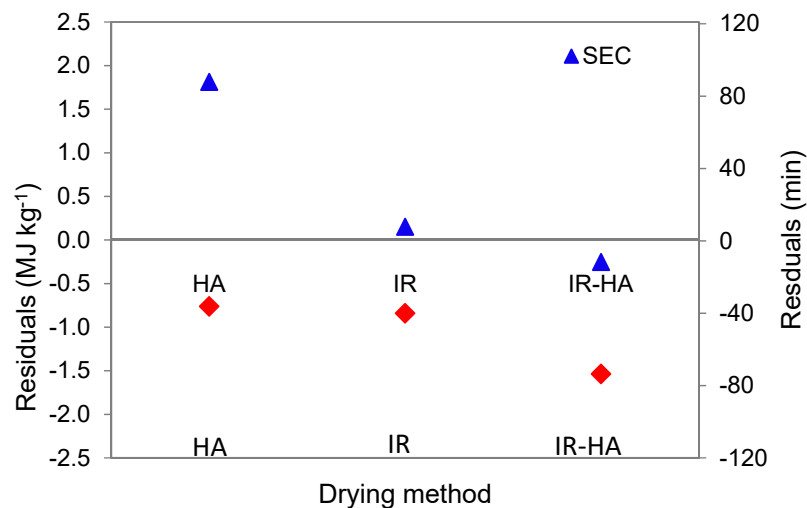


Figure 6. The residual plot of minimum drying time and corresponding specific energy consumption (SEC) using the generated equations using the studied drying systems; hot air convection drying (HA) at 60 °C and 1.0 m/s, infrared radiation drying (IR) at 0.3 W/cm², and 0.5 m/s and combined infrared-hot air convection (IR-HA) at 60 °C, 0.3 W/cm², and 0.5 m/s.

3.4. Overall Comparison

The lowest drying time using each of the three systems studied, where combined drying (IR-HA) showed the lowest significant drying time of 225 min at 60 °C, 0.3 W/cm², and 0.5 m/s, which was 40.8% and 29.7% lower than hot air convection and IR, respectively (Figure 7A). However, IR showed a significant reduction of 15.8% in drying time with respect to hot air convection. The lowest recorded SEC values for biomass dried using different systems are presented in Figure 7B. A minimum SEC of 3.77 MJ/kg was recorded using combined IR-hot air convection drying, which was 91.7% and 51.7% lower than the hot air convection and IR, respectively. The observed energy consumption using the combined dryer in the present study showed lower values in comparison to previous studies by other researchers (Table 1). For example, the SEC in the present study was 91.3% lower than that of hot air convection drying of onion [51], and 93.9% lower than combined microwave and hot air convection drying of garlic cloves [52]. Thus, the present study suggested a combined IR and hot air convection drying at 60 °C, 0.3 W/cm², and 0.5 m/s as optimum conditions for efficient drying of biomass with high water content.

Although derived from composting, the drying of bio-wastes has been extensively studied for many purposes, such as energy recovery, bio-chemicals, and bio-fertilizer production [53]. Composting aims at producing a stabilized, safe and nutrient-enriched soil fertilizer with humic substance formation during microbial metabolism [54]. However, removing the excess water from bio-wastes is the principal target of drying, by which a solid biomass with high energy content or powdered biomass can be obtained [55]. The composting process depends mainly on the growth of microbes which is affected by environmental conditions. On the other hand, drying is much faster compared to composting which makes it more practical for large scale applications. Therefore, drying is a prospective and profitable technique for biomass treatment. The economic costs of drying can be calculated as both operating and ownership costs, while the energy cost is the main aspect of the present study. The three studied drying systems use electricity to power fans, light the IR and to provide heat. In the present study, moisture decreased from approximately 95% to 5%, i.e., an average electricity usage of 0.14, 0.02 and 0.01 kWh per point of moisture removed using HA, IR and the combined system, respectively. Shouse et al. [56] estimated an average electricity usage of 0.01 kWh per point of moisture removed per bushel for high-temperature systems, and up to 0.40 kWh per point removed for natural air-drying systems which use only electricity. Thus, using the combined system in the present study showed high drying efficiency. According to the US Energy Information Administration [57], the current electricity

price is US\$ 0.13 /kWh. Based on the SEC, the estimated cost for drying 1 ton could be calculated as US\$ 2.51, 0.28 and 0.14 for HA, IR, and the combined system, respectively (Figure 7B). Further, for per point of moisture removed, the estimated cost could be 2.79, 0.31 and 0.15 cents for the three studied systems, respectively. These results confirm the efficiency of the combined system in a large scale application of biomass drying. However, further comparable studies using the suggested conditions on different biomass feedstock is of great importance.

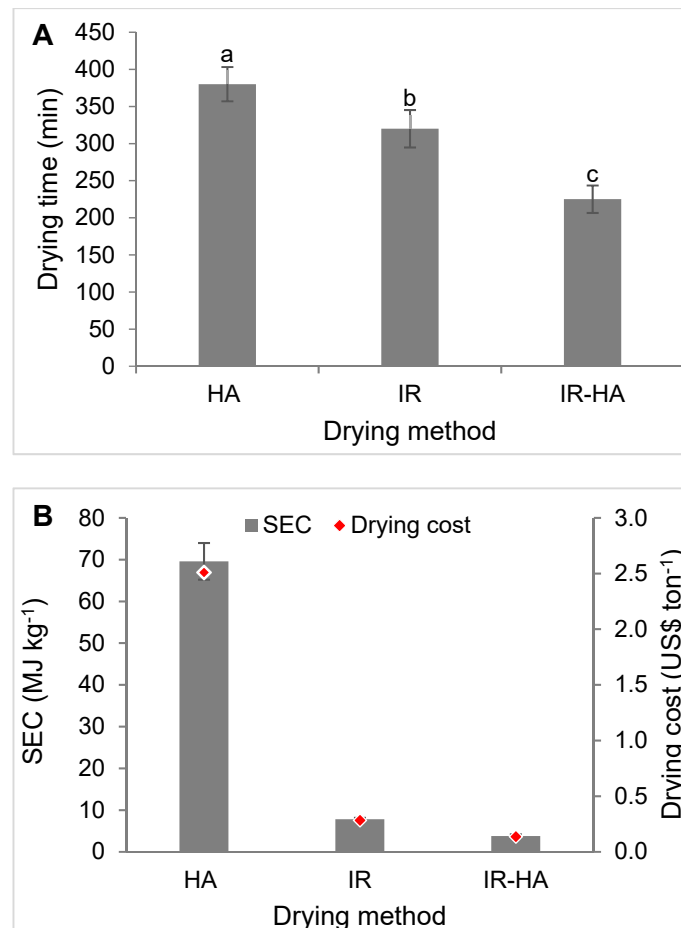


Figure 7. The minimum drying time (A) and corresponding specific energy consumption (SEC, B) recorded using different studied drying systems; hot air convection drying (HA) at 60 °C and 1.0 m/s, infrared radiation drying (IR) at 0.3 W/cm², and 0.5 m/s and combined infrared-hot air convection (IR-HA) at 60 °C, 0.3 W/cm², and 0.5 m/s. The columns with the same letter showed insignificant differences (at $P \leq 0.05$).

Table 1. A comparison between the results obtained in this study and that from the literature when considering the minimum required time (MRT) and specific energy consumption (SEC) for drying different biomasses when applying the combined infrared-hot air convection drying system.

Agricultural Products	Drying Method	Drying Conditions	MRT (hours)	SEC	Final Moisture Content (%)	References
Garlic cloves	HA	$T = 70, V = 2$	6.5	85.45 MJ/kg	6	[52]
	MW-HA	$T = 70, V = 2, W = 40$	1	62.02 MJ/kg	6	
Carrot slices	MW-VA	$W = 2.4, VA = 5$	1.6	50 KJ/kg	8	[58]
Red pepper	HA	$T = 70, V = 1.5$	2.66	4.45 KJ/kg	10	[59]
Jujube	HA	$T = 70, V = 1.5$	16.6	203.59 KWh/kg	12	[60]
Apple	HA	$T = 150, V = 1$	1.18	500 KWh/kg	12	[61]
	IR	$IR = 0.49, V = 1$	1	70 KWh/kg	12	
Apple	HA	$T = 60, V = 0.6$	5.6	24 MJ/kg	11	[62]
	IR	$IR = 2000, V = 0.6$	4	7 MJ/kg	11	
	IR-HA	$T = 60, V = 0.6, IR = 2000$	2.5	5 MJ/kg	11	
Onion	HA	$T = 70, V = 2$	9.2	43.34 MJ/kg	10	[51]
Tomato slices	IR-HA	$T = 60, V = 0.3, IR = 300$	3.75	3.77 MJ/kg	5	This study

HA = hot air convection; MW = Microwave drying; IR = Infrared; MW-HA = combination of microwave and convection hot air; IR-HA = combination of infrared and convection hot air; T = air temperature ($^{\circ}\text{C}$); V = air velocity (m/s); VA = the vacuum pressure (KPa); W = Microwave power; IR = Infrared intensity (W/m^2).

4. Conclusions

The present study evaluated three drying systems, namely hot air convection, IR, and a combined IR-HA for the drying of tomato slices as a model high water content biomass. The results showed that the highest drying time was recorded using the hot air convection system, while the combined system showed the lowest drying time and, consequently, the lowest SEC. The higher temperatures and/or IR radiation played a significant role in reducing the drying time and the SEC. However, increasing the air velocity negatively increased the drying time and the SEC in all the studied systems. To minimize the energy consumption and the duration of the drying process, the present study suggested IR radiation combined with hot air at a low air velocity. Further studies on the economic feasibility of the application of such a system for biomass drying, as well as the impact of drying on the thermal behaviors of the biomass, need additional investigation.

Supplementary Materials: The following are available online at <http://www.mdpi.com/1996-1073/12/14/2818/s1>, Figure S1: Variation of drying time due to change in the drying temperature and drying air velocity using a hot air convection dryer, Figure S2: The rate of reduction in the drying time at different temperatures (A, compared to the drying time at 40°C) and at different air velocities (B, compared to the drying time at 0.5 m/s), Figure S3: Interaction effect of temperature and air velocity on specific energy consumption using a hot air convection dryer, Figure S4: Variation of drying time due to change in the drying temperature and drying air velocity using an infrared dryer, Figure S5: Interaction effect of infrared intensity and air velocity on specific energy consumption using infrared drying, Figure S6: Variation of drying time due to changes in infrared radiation intensity at different air velocities using a combined infrared/hot air convection dryer at 40°C (A), 50°C (B) and 60°C (C), Figure S7: Variation of specific energy consumption due to changes in infrared radiation intensity at different air velocities using a combined infrared/hot air convection dryer at 40°C (A), 50°C (B) and 60°C (C).

Author Contributions: Conceptualization, H.S.E.-M.; data curation, H.S.E.-M.; formal analysis, H.S.E.-M.; funding acquisition, B.-H.J.; investigation, H.S.E.-M.; methodology, H.S.E.-M.; software, H.S.E.-M.; validation, A.E.-F.A., C.-U.K., J.-K.C., B.B. and B.-H.J.; writing—original draft, H.S.E.-M.; writing—review and editing, A.E.-F.A., C.-U.K., J.-K.C., B.B. and B.-H.J.

Funding: This work was financially funded by Egyptian Ministry of Higher Education and Scientific Research (MHESR), Egypt; the Priority Academic Program Development of Jiangsu Higher Education Institutions, China; and Mid-Career Researcher Program (No. 2017R1A2B2004143) of the National Research Foundation of Korea (NRF), Republic of Korea.

Acknowledgments: We acknowledge the Egyptian Ministry of Higher Education and Scientific Research (MHESR), Egypt and the Priority Academic Program Development of Jiangsu Higher Education Institutions, China for financial support. Authors are also thankful for the financial support from Mid-Career Researcher Program (No. 2017R1A2B2004143) of the National Research Foundation of Korea (NRF), Republic of Korea.

Conflicts of Interest: The authors declare no conflicts of interest.

References

1. Dev, S.; Saha, S.; Kurade, M.B.; Salama, E.S.; El-Dalatony, M.M.; Ha, G.S.; Chang, S.W.; Jeon, B.H. Perspective on anaerobic digestion for biomethanation in cold environments. *Renew. Sustain. Energy Rev.* **2019**, *103*, 85–95. [[CrossRef](#)]
2. Brigham, C.J.; Riedel, S.L. The potential of polyhydroxyalkanoate production from food wastes. *Appl. Food Biotechnol.* **2019**, *6*, 12.
3. Pratt, S.; Vandi, L.J.; Gapes, D.; Werker, A.; Oehmen, A.; Laycock, B. Polyhydroxyalkanoate (PHA) bioplastics from organic waste. In *Biorefinery: Integrated Sustainable Processes for Biomass Conversion to Biomaterials, Biofuels, and Fertilizers*; Bastidas-Oyanedel, J.R., Schmidt, J.E., Eds.; Springer International Publishing: Cham, Switzerland, 2019; pp. 615–638.
4. Tsang, Y.F.; Kumar, V.; Samadar, P.; Yang, Y.; Lee, J.; Ok, Y.S.; Song, H.; Kim, K.H.; Kwon, E.E.; Jeon, Y.J. Production of bioplastic through food waste valorization. *Environ. Int.* **2019**, *127*, 625–644. [[CrossRef](#)] [[PubMed](#)]
5. Moreira, J.R. Global biomass energy potential. *Mitig. Adapt. Strateg. Glob. Change* **2006**, *11*, 313–342. [[CrossRef](#)]
6. Uzoejinwa, B.B.; He, X.; Wang, S.; El-Fatah Abomohra, A.; Hu, Y.; Wang, Q. Co-pyrolysis of biomass and waste plastics as a thermochemical conversion technology for high-grade biofuel production: Recent progress and future directions elsewhere worldwide. *Energy Convers. Manag.* **2018**, *163*, 468–492. [[CrossRef](#)]
7. Kumar, A.; Kumar, K.; Kaushik, N.; Sharma, S.; Mishra, S. Renewable energy in India: Current status and future potentials. *Renew. Sustain. Energy Rev.* **2010**, *14*, 2434–2442. [[CrossRef](#)]
8. Ramos-Suárez, J.L.; Martínez, A.; Carreras, N. Optimization of the digestion process of *Scenedesmus* sp. and *Opuntia maxima* for biogas production. *Energy Convers. Manag.* **2014**, *88*, 1263–1270. [[CrossRef](#)]
9. Chang, S.E.; Saha, S.; Kurade, M.B.; Salama, E.S.; Chang, S.W.; Jang, M.; Jeon, B.-H. Improvement of acidogenic fermentation using an acclimatized microbiome. *Int. J. Hydrog. Energy* **2018**, *43*, 22126–22134. [[CrossRef](#)]
10. Basak, B.; Fatima, A.; Jeon, B.H.; Ganguly, A.; Chatterjee, P.K.; Dey, A. Process kinetic studies of biohydrogen production by co-fermentation of fruit-vegetable wastes and cottage cheese whey. *Energy Sustain. Dev.* **2018**, *47*, 39–52. [[CrossRef](#)]
11. Abomohra, A.E.F.; Jin, W.; El-Sheekh, M. Enhancement of lipid extraction for improved biodiesel recovery from the biodiesel promising microalga *Scenedesmus obliquus*. *Energy Convers. Manag.* **2016**, *108*, 23–29. [[CrossRef](#)]
12. El-Dalatony, M.M.; Salama, E.S.; Kurade, M.B.; Kim, K.Y.; Govindwar, S.P.; Kim, J.R.; Kwon, E.E.; Min, B.; Jang, M.; Oh, S.E.; et al. Whole conversion of microalgal biomass into biofuels through successive high-throughput fermentation. *Chem. Eng. J.* **2019**, *360*, 797–805. [[CrossRef](#)]
13. De Farias Silva, C.E.; Bertucco, A. Bioethanol from microalgae and cyanobacteria: A review and technological outlook. *Process Biochem.* **2016**, *51*, 1833–1842. [[CrossRef](#)]
14. El-Dalatony, M.M.; Saha, S.; Govindwar, S.P.; Abou-Shanab, R.A.I.; Jeon, B.H. Biological conversion of amino acids to higher alcohols. *Trends Biotechnol.* **2019**, *37*, 855–869. [[CrossRef](#)] [[PubMed](#)]
15. Wang, S.; Uzoejinwa, B.B.; Abomohra, A.E.-F.; Wang, Q.; He, Z.; Feng, Y.; Zhang, B.; Hui, C.W. Characterization and pyrolysis behavior of the green microalga *Micractinium conductrix* grown in lab-scale tubular photobioreactor using Py-GC/MS and TGA/MS. *J. Anal. Appl. Pyrolysis* **2018**, *135*, 340–349. [[CrossRef](#)]
16. Wang, S.; Yerkebulan, M.; Abomohra, A.E.F.; El-Khodary, S.; Wang, Q. Microalgae harvest influences the energy recovery: A case study on chemical flocculation of *Scenedesmus obliquus* for biodiesel and crude bio-oil production. *Bioresour. Technol.* **2019**, *286*, 121371. [[CrossRef](#)] [[PubMed](#)]
17. Sharifzadeh, M.; Sadeqzadeh, M.; Guo, M.; Borhani, T.N.; Murthy Konda, N.V.S.N.; Garcia, M.C.; Wang, L.; Hallett, J.; Shah, N. The multi-scale challenges of biomass fast pyrolysis and bio-oil upgrading: Review of the state of art and future research directions. *Prog. Energy Combust. Sci.* **2019**, *71*, 1–80. [[CrossRef](#)]
18. Chen, L.; Xing, L.; Han, L. Renewable energy from agro-residues in China: Solid biofuels and biomass briquetting technology. *Renew. Sustain. Energy Rev.* **2009**, *13*, 2689–2695. [[CrossRef](#)]
19. Ståhl, M.; Granström, K.; Berghel, J.; Renström, R. Industrial processes for biomass drying and their effects on the quality properties of wood pellets. *Biomass Bioenergy* **2004**, *27*, 621–628. [[CrossRef](#)]

20. Cai, J.; Chen, S. Determination of drying kinetics for biomass by thermogravimetric analysis under nonisothermal condition. *Dry. Technol.* **2008**, *26*, 1464–1468. [[CrossRef](#)]
21. Anderson, J.-O.; Westerlund, L. Improved energy efficiency in sawmill drying system. *Appl. Energy* **2014**, *113*, 891–901. [[CrossRef](#)]
22. Dai, J.W.; Rao, J.Q.; Wang, D.; Xie, L.; Xiao, H.W.; Liu, Y.H.; Gao, Z.-J. Process-based drying temperature and humidity integration control enhances drying kinetics of apricot halves. *Dry. Technol.* **2015**, *33*, 365–376. [[CrossRef](#)]
23. Lamidi, R.O.; Jiang, L.; Pathare, P.B.; Wang, Y.D.; Roskilly, A.P. Recent advances in sustainable drying of agricultural produce: A review. *Appl. Energy* **2019**, *233–234*, 367–385. [[CrossRef](#)]
24. Hu, Y.; Wang, S.; Li, J.; Wang, Q.; He, Z.; Feng, Y.; Abomohra, A.E.F.; Afonaa-Mensah, S.; Hui, C. Co-pyrolysis and co-hydrothermal liquefaction of seaweeds and rice husk: Comparative study towards enhanced biofuel production. *J. Anal. Appl. Pyrolysis* **2018**, *129*, 162–170. [[CrossRef](#)]
25. Wang, X.; Chen, H.; Luo, K.; Shao, J.; Yang, H. The Influence of Microwave Drying on Biomass Pyrolysis. *Energy Fuels* **2008**, *22*, 67–74. [[CrossRef](#)]
26. Rathore, N.S.; Panwar, N.L. Experimental studies on hemi cylindrical walk-in type solar tunnel dryer for grape drying. *Appl. Energy* **2010**, *87*, 2764–2767. [[CrossRef](#)]
27. Singh, P.L. Silk cocoon drying in forced convection type solar dryer. *Appl. Energy* **2011**, *88*, 1720–1726. [[CrossRef](#)]
28. Chua, K.J.; Chou, S.K. Low-cost drying methods for developing countries. *Trends Food Sci. Technol.* **2003**, *14*, 519–528. [[CrossRef](#)]
29. Zhang, M.; Chen, H.; Mujumdar, A.S.; Tang, J.; Miao, S.; Wang, Y. Recent developments in high-quality drying of vegetables, fruits, and aquatic products. *Crit. Rev. Food Sci. Nutr.* **2017**, *57*, 1239–1255. [[CrossRef](#)]
30. Onwude, D.I.; Hashim, N.; Chen, G. Recent advances of novel thermal combined hot air drying of agricultural crops. *Trends Food Sci. Technol.* **2016**, *57*, 132–145. [[CrossRef](#)]
31. Elsayed, M.; Abomohra, A.E.F.; Ai, P.; Wang, D.; El-Mashad, H.M.; Zhang, Y. Biorefining of rice straw by sequential fermentation and anaerobic digestion for bioethanol and/or biomethane production: Comparison of structural properties and energy output. *Bioresour. Technol.* **2018**, *268*, 183–189. [[CrossRef](#)]
32. Elsayed, M.; Abomohra, A.E.F.; Ai, P.; Jin, K.; Fan, Q.; Zhang, Y. Acetogenesis and methanogenesis liquid digestates for pretreatment of rice straw: A holistic approach for efficient biomethane production and nutrient recycling. *Energy Convers. Manag.* **2019**, *195*, 447–456. [[CrossRef](#)]
33. Wang, S.; Cao, B.; Feng, Y.; Sun, C.; Wang, Q.; Abomohra, A.E.-F.; Afonaa-Mensah, S.; He, Z.; Zhang, B.; Qian, L.; et al. Co-pyrolysis and catalytic co-pyrolysis of *Enteromorpha clathrata* and rice husk. *J. Therm. Anal. Calorim.* **2019**, *135*, 2613–2623. [[CrossRef](#)]
34. El-Sheekh, M.; Abomohra, A.E.F.; Eladel, H.; Battah, M.; Mohammed, S. Screening of different species of *Scenedesmus* isolated from Egyptian freshwater habitats for biodiesel production. *Renew. Energy* **2018**, *129*, 114–120. [[CrossRef](#)]
35. Han, S.; Jin, W.; Chen, Y.; Tu, R.; Abomohra, A.E.F. Enhancement of lipid production of *Chlorella Pyrenoidosa* cultivated in municipal wastewater by magnetic treatment. *Appl. Biochem. Biotechnol.* **2016**, *180*, 1043–1055. [[CrossRef](#)] [[PubMed](#)]
36. Chayjan, R.A.; Salari, K.; Abedi, Q.; Sabziparvar, A.A. Modeling moisture diffusivity, activation energy and specific energy consumption of squash seeds in a semi fluidized and fluidized bed drying. *J. Food Sci. Technol.* **2013**, *50*, 667–677. [[CrossRef](#)] [[PubMed](#)]
37. Doymaz, İ. Air-drying characteristics of tomatoes. *J. Food Eng.* **2007**, *78*, 1291–1297. [[CrossRef](#)]
38. Contreras, C.; Martín-Esparza, M.E.; Chiralt, A.; Martínez-Navarrete, N. Influence of microwave application on convective drying: Effects on drying kinetics, and optical and mechanical properties of apple and strawberry. *J. Food Eng.* **2008**, *88*, 55–64. [[CrossRef](#)]
39. Khir, R.; Pan, Z.; Salim, A.; Hartsough, B.R.; Mohamed, S. Moisture diffusivity of rough rice under infrared radiation drying. *LWT Food Sci. Technol.* **2011**, *44*, 1126–1132. [[CrossRef](#)]
40. Sharma, G.P.; Verma, R.C.; Pathare, P.B. Thin-layer infrared radiation drying of onion slices. *J. Food Eng.* **2005**, *67*, 361–366. [[CrossRef](#)]
41. Adabi, E.M.; Motevali, A.; Nikbakht, A.M.; Khoshtaghaza, H.M. Investigation of some pretreatments on energy and specific energy consumption drying of black mulberry. *Chem. Ind. Chem. Eng.* **2013**, *19*, 89–105. [[CrossRef](#)]

42. Onwude, D.I.; Hashim, N.; Abdan, K.; Janius, R.; Chen, G. The effectiveness of combined infrared and hot-air drying strategies for sweet potato. *J. Food Eng.* **2019**, *241*, 75–87. [[CrossRef](#)]
43. Das, I.; Das, S.K.; Bal, S. Drying kinetics of high moisture paddy undergoing vibration-assisted infrared (IR) drying. *J. Food. Eng.* **2009**, *95*, 166–171. [[CrossRef](#)]
44. Ruiz Celma, A.; Rojas, S.; Lopez-Rodríguez, F. Mathematical modelling of thin-layer infrared drying of wet olive husk. *Chem. Eng. Process. Process Intensif.* **2008**, *47*, 1810–1818. [[CrossRef](#)]
45. Fasina, O.; Tyler, B.; Pickard, M.; Zheng, G.H.; Wang, N. Effect of infrared heating on the properties of legume seeds. *Int. J. Food Sci. Technol.* **2001**, *36*, 79–90. [[CrossRef](#)]
46. Jaturonglumlert, S.; Kiatsiriroat, T. Heat and mass transfer in combined convective and far-infrared drying of fruit leather. *J. Food Eng.* **2010**, *100*, 254–260. [[CrossRef](#)]
47. Lin, Y.L.; Li, S.J.; Zhu, Y.; Bingol, G.; Pan, Z.; McHugh, T.H. Heat and mass transfer modeling of apple slices under simultaneous infrared dry blanching and dehydration process. *Dry. Technol.* **2009**, *27*, 1051–1059. [[CrossRef](#)]
48. Mongpraneet, S.; Abe, T.; Tsurusaki, T. Accelerated drying of welsh onion by far infrared radiation under vacuum conditions. *J. Food Eng.* **2002**, *55*, 147–156. [[CrossRef](#)]
49. Liu, Y.; Zhu, W.; Luo, L.; Li, X.; Yu, H. A mathematical model for vacuum far-infrared drying of potato slices. *Dry. Technol.* **2014**, *32*, 180–189. [[CrossRef](#)]
50. Zhang, M.; Tang, J.; Mujumdar, A.S.; Wang, S. Trends in microwave-related drying of fruits and vegetables. *Trends Food Sci. Technol.* **2006**, *17*, 524–534. [[CrossRef](#)]
51. El-Mesery, H.S.; Mwithiga, G. Comparison of a gas fired hot-air dryer with an electrically heated hot-air dryer in terms of drying process, energy consumption and quality of dried onion slices. *Afr. J. Agric. Res.* **2012**, *7*, 4440–4452.
52. Sharma, G.P.; Prasad, S. Specific energy consumption in microwave drying of garlic cloves. *Energy* **2006**, *31*, 1921–1926. [[CrossRef](#)]
53. Ma, J.; Zhang, L.; Mu, L.; Zhu, K.; Li, A. Thermally assisted bio-drying of food waste: Synergistic enhancement and energetic evaluation. *Waste Manage.* **2018**, *80*, 327–338. [[CrossRef](#)] [[PubMed](#)]
54. Sharholly, M.; Ahmad, K.; Mahmood, G.; Trivedi, R.C. Municipal solid waste management in Indian cities—A review. *Waste Manage.* **2008**, *28*, 459–467. [[CrossRef](#)] [[PubMed](#)]
55. Tom, A.P.; Pawels, R.; Haridas, A. Biodrying process: A sustainable technology for treatment of municipal solid waste with high moisture content. *Waste Manage.* **2016**, *49*, 64–72. [[CrossRef](#)] [[PubMed](#)]
56. Shouse, S.; Hanna, M.; Petersen, D. Energy considerations for low-temperature grain drying. In *Agriculture and Environment Extension Publications*; Outreach, I., Ed.; Iowa Energy Center: Ames, IA, USA, 2012; Volume 200.
57. USEIA Average Price of Electricity to Ultimate Customers by End-Use sSector, by State, April 2019, U.S. Energy Information Administration. Available online: https://www.eia.gov/electricity/monthly/epm_table_grapher.php?t=epmt_5_6_a (accessed on 11 July 2019).
58. Yan, W.Q.; Zhang, M.; Huang, L.L.; Tang, J.; Mujumdar, A.S.; Sun, J.C. Studies on different combined microwave drying of carrot pieces. *Int. J. Food Sci. Technol.* **2010**, *45*, 2141–2148. [[CrossRef](#)]
59. Akpınar, E.K. Energy and exergy analyses of drying of red pepper slices in a convective type dryer. *Int. Commun. Heat Mass Transf.* **2004**, *31*, 1165–1176. [[CrossRef](#)]
60. Abbaszadeh Mayvan, A.; Ghobadian, B. Effective moisture diffusivity, activation energy and energy consumption in thin-layer drying of Jujube (*Zizyphus jujube* Mill). *J. Agric. Sci. Technol.* **2012**, *14*, 523–533.
61. Samadi, S.H.; Loghmanieh, I. Evaluation of energy aspects of apple drying in the hot-air and infrared dryers. *Energy Res. J.* **2013**, *4*, 30–38. [[CrossRef](#)]
62. El-Mesery, H.S.; Mwithiga, G. Performance of a convective, infrared and combined infrared—Convective heated conveyor-belt dryer. *J. Food Sci. Technol.* **2015**, *52*, 2721–2730. [[CrossRef](#)]

